Numerical modeling of nonlinear modulation of coda wave interferometry in a multiple scattering medium with the presence of a localized micro-cracked zone

Guangzhi Chen, Damien Pageot, Jean-Baptiste Legland, Odile Abraham, Mathieu Chekroun, Vincent Tournat

Numerical modeling of nonlinear modulation of coda wave interferometry in a multiple scattering medium with the presence of a localized micro-cracked zone

Guangzhi Chen, Damien Pageot, Jean-Baptiste Legland, Odile Abraham, Mathieu Chekroun, and Vincent Tournat

Citation: AIP Conference Proceedings **1949**, 210002 (2018); doi: 10.1063/1.5031645
View online: https://doi.org/10.1063/1.5031645
View Table of Contents: http://aip.scitation.org/toc/apc/1949/1
Published by the American Institute of Physics

Numerical modeling of Nonlinear modulation of Coda Wave Interferometry in a multiple scattering medium with the presence of a localized micro-cracked zone

Guangzhi Chen[1, 2, a)], Damien Pageot [1, b)], Jean-Baptiste Legland [1, c)], Odile Abraham[1,d)], Mathieu Chekroun [2, e)], Vincent Tournat [2, f)]

[1]*IFSTTAR, Dep. GERS, Lab. GeoEND, CS4, F-44344, Bouguenais Cedex, France*
[2]*LUNAM University, LAUM, CNRS UMR 6613, University du Maine, Av. O. Messiaen, 72085 Le Mans Cedex, France.*

[a)]Corresponding author: guangzhi.chen@ifsttar.fr
[b)]damien.pageot@ifsttar.fr
[c)]jean-baptiste.legland@ifsttar.fr
[d)]odile.abraham@ifsttar.fr
[e)]mathieu.chekroun@univ-lemans.fr
[f)]vincent.tournat@univ-lemans.fr

Abstract. The spectral element method is used to perform a parametric sensitivity study of the nonlinear coda wave interferometry (NCWI) method in a homogeneous sample with localized damage [1]. The influence of a strong pump wave on a localized nonlinear damage zone is modeled as modifications to the elastic properties of an effective damage zone (EDZ), depending on the pump wave amplitude. The local change of the elastic modulus and the attenuation coefficient have been shown to vary linearly with respect to the excitation amplitude of the pump wave as in previous experimental studies of Zhang et al. [2]. In this study, the boundary conditions of the cracks, i.e. clapping effects is taken into account in the modeling of the damaged zone. The EDZ is then modeled with random cracks of random orientations, new parametric studies are established to model the pump wave influence with two new parameters: the change of the crack length and the crack density. The numerical results reported constitute another step towards quantification and forecasting of the nonlinear acoustic response of a cracked material, which proves to be necessary for quantitative non-destructive evaluation.

INTRODUCTION

Various nonlinear ultrasonic testing methods reported in the last decades have shown high sensitivity and great efficiency in detecting small amount of damage in complex materials [3-5]. Especially those based on the non-classical nonlinearities, including harmonic generation [6,7], Nonlinear Elastic Wave Spectroscopy (NEWS) and Nonlinear Resonance Ultrasound Spectroscopy (NRUS) [8,9], nonlinear modulation [2, 10], Dynamic Acousto-Elasticity Testing (DAET) [11,12], provide a mean for detecting early damage or micro-cracks with the change in the nonlinear elastic parameters, while the linear elastic parameters remain unchanged. Another set of methods widely studied recently for non-destructive testing and evaluation (NDT&E) of complex materials is called Coda Wave Interferometry (CWI) [13, 14]. The coda wave contains abundant information on the medium and it is shown to be reproducible [14] with a very high sensitivity to disturbances of the propagation medium [15-17]. On this basis, a new set of methods, combining the Nonlinear modulation method and the Coda Wave Interferometry (NCWI for Nonlinear Coda Wave Interferometry) was proposed by Zhang et al. in 2013 for glass [2] and applied to cracked mortar samples by Hilloulin et al. [10].

44th Annual Review of Progress in Quantitative Nondestructive Evaluation, Volume 37
AIP Conf. Proc. 1949, 210002-1–210002-7; https://doi.org/10.1063/1.5031645
Published by AIP Publishing. 978-0-7354-1644-4/$30.00

The CWI method consists of comparing two signals coming from two different material states, including a reference state and a relative damaged state. Two observables to estimate the differences between the two mentioned signals are: the relative variation of velocity θ and the remnant decorrelation coefficient Kd. A recent and powerful tool to estimate the change in propagation velocity is called Stretching. It evaluates the correlation coefficient between a perturbed signal and a reference signal, at an expansion rate (k = 1,2,…,n for different levels of expansion) that simulates a global increase/decrease in propagation velocity within the medium [14].

$$CC(\theta_k) = \frac{\int_{t_c-T}^{t_c+T} u_r(t(1+\theta_k))u_p(t)dt}{\sqrt{\int_{t_c-T}^{t_c+T} u_r^2(t(1+\theta_k))dt \int_{t_c-T}^{t_c+T} u_p^2(t)dt}} \quad (1)$$

The value of the correlation coefficient $CC(\theta_k)$ in Eq. (1) represents, quantitatively, the similarity of the two signals recorded before and after perturbation of the medium within a selected time window $[t_c\text{-}T, t_c\text{+}T]$, where t_c is the central time of the window and 2T the length of the analyzed window. Herein, two CWI observables are traditionally introduced: i) when $CC(\theta_k)$ reaches its maximum value, the relative variation in effective coda velocity is introduced and simply denoted as $\theta = \theta_k = \delta v/v$; and ii) in order to quantify the level of distortion between the two signals, the remnant decorrelation coefficient Kd is introduced as $Kd = 100\ (1 - CC(\theta))$.

The quadratic hysteresis nonlinearity has been demonstrated in the experiment of Zhang *et al.* [2] by using a pump wave of large amplitude which is increased step by step. In order to study the effect of the pump wave in the experiment, numerical modeling has been done for each level of the pump wave amplitude, the state of the damaged zone has been modeled by changes in the local intrinsic elastic properties of the material [1]. The relationship between the amplitude of the pump wave in the experiment and the changes in elastic properties of the damaged zone was thus established [1]. In this study, a new modeling of the effective damaged zone in the material is considered: random cracks of random orientations are added in the damaged zone of the numerical models so that the numerical model becomes more realistic.

NUMERICAL CONFIGURATIONS

The numerical modeling is realized using the two-dimensional spectral element method (SEM 2D) [18] and the meshes are made using the GMSH software. Five numerical configurations are developed as shown in Fig. 1, each one containing a different number of cracks ranging from 4 to 20. The matrix size is set to 200×200 mm^2, the random cracks of random orientations in the models are generated within a circular effective damaged zone (EDZ) and the center of the EDZ is located at (155 mm, 140 mm). Each crack is modeled by an empty mesh cell with a thickness of 10^{-2} mm, which is negligible in front of the minimum wavelength 4.2 mm (Fig. 2). The size of each crack is set at 10 mm × 0.01 mm, hence the crack aspect ratio is equal to 10^{-3} which generally corresponds to an open crack in reality [19]. The purpose of putting the void in the cracks is to maximize the contrast between the matrix and the cracks, the waves will be completely reflected in front of the cracks, which corresponds to the case of open cracks. The emission source is a chirp signal with the frequency band of [200 kHz, 800 kHz] at (50 mm, 200 mm). The duration of the source is 0.2 ms.

The characteristics of the medium for all numerical models, are assigned the following properties: the matrix (glass) has a Young's modulus E_{mtx} = 69 GPa, a Poisson's ratio ν_{mtx} = 0.25 and a volumetric mass density ρ_{mtx} = 2500 $kg{\cdot}m^{-3}$, yielding the velocities for P-wave of 5755 $m{\cdot}s^{-1}$ and S-wave of 3323 $m{\cdot}s^{-1}$. The quality factors for Q_λ^{-1} and Q_μ^{-1} are respectively 1250 and 350 [1].

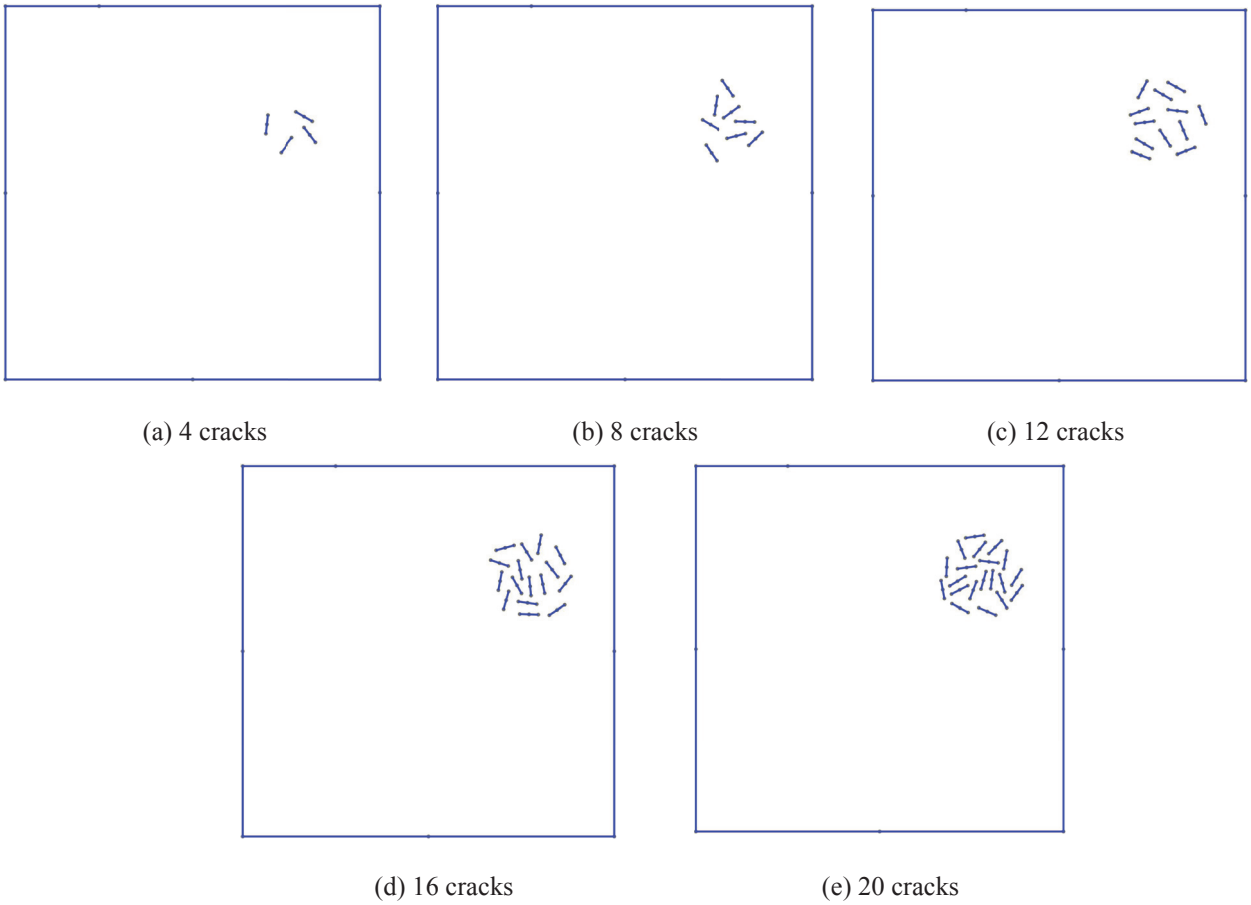

FIGURE 1. Numerical configurations of damaged material with random cracks in a circular effective damaged zone (EDZ) located at (155 mm, 140 mm), each model contains a different number of cracks ranging from 4 to 20. The blue lines represent the contour of the matrix and the cracks. The matrix size equals to 200×200 mm^2. The source position is (50 mm, 200 mm).

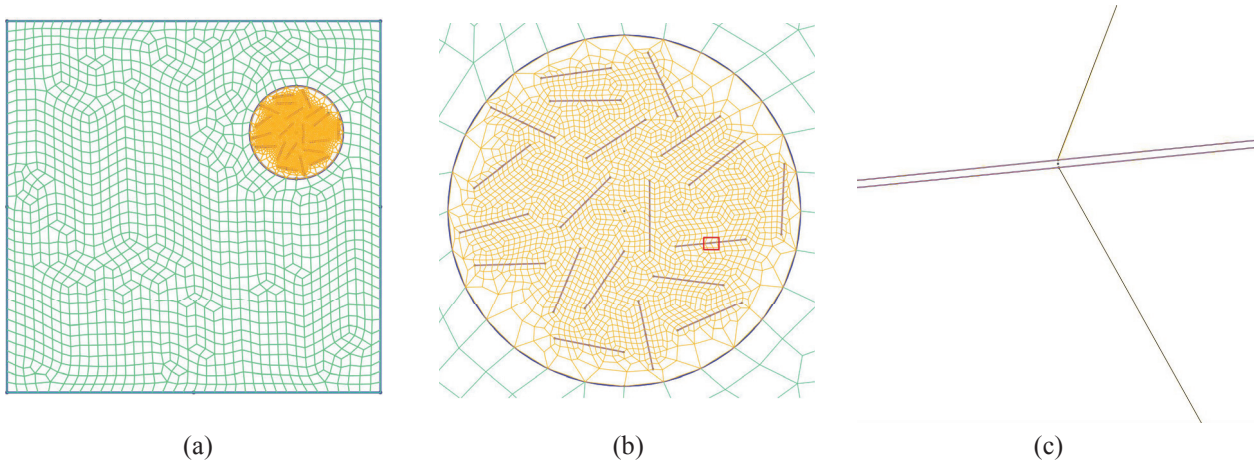

FIGURE 2. Example of the mesh for a homogeneous model with an Effective Damage Zone (EDZ) filled with 20 random cracks of random orientations. Each crack is modeled by one void cell, with a size of 10 mm × 0.01 mm. The blue lines represent the contour of the matrix, the EDZ and the cracks. (a) Mesh of the numerical model; (b) Zoom of the meshed EDZ; (c) Zoom of one crack corresponding to the red marks in (b).

NUMERICAL RESULTS

Different damaged states of the material are simulated by small changes in the crack length and CWI observables (the relative variation in velocity θ and the remnant decorrelation coefficient Kd) are evaluated for each of them. Changes in the crack length are identically applied at the same time to all existing cracks in the material: $\Delta L = (L_{damage} - L_{initial}) / L_{initial}$ varies between 0 and +1.8%, where ΔL = 0 corresponds to the reference model. Fig. 3 shows an example of temporal signals for the numerical model with 4 random cracks. The blue line corresponds to the reference model without change of the crack length (ΔL = 0), while the green line indicates the damaged state of the material with ΔL = +1.8%.

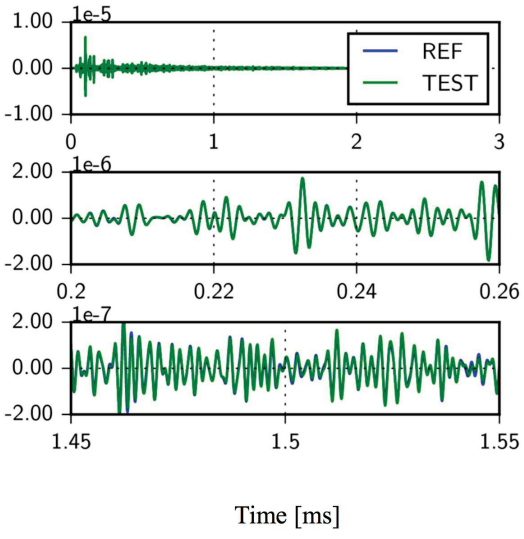

FIGURE 3. Example of temporal signals for the model with 4 random cracks. The blue line corresponds to the reference model without change of the crack length (ΔL = 0), while the green line indicates the damaged state of the material with ΔL = +1.8%.

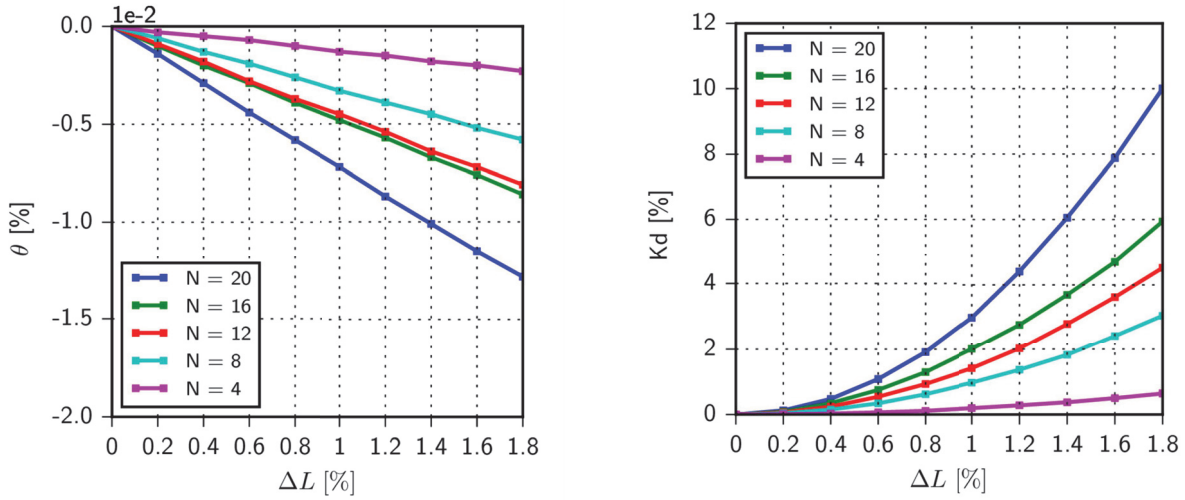

(a) (b)

FIGURE 4. CWI observables vs. changes in the crack length (ΔL). Five numerical models are used, each one with a fixed number of random cracks, ranging from 4 to 20: (a) Relative variation of velocity θ vs. ΔL; (b) Remnant decorrelation coefficient Kd vs. ΔL.

In Fig. 4 (a), for all five models with a different number of cracks, a linear dependence is observed between θ and ΔL for low levels of crack length change. This decrease in the relative variation of velocity may be related to a global loss of rigidity of the material and also to surface waves behavior. The velocity of the coda waves is an average velocity which contains all type of waves; with more surface waves generated along the two crack surfaces, the average velocity will be lowered. The slope of the linear function connecting θ with ΔL is denoted by α_θ^L (Eq. 2).

$$\theta = \alpha_\theta^L \cdot \Delta L \qquad (2)$$

Also, as shown in Fig. 4 (b), a quadratic dependence is clearly observed between Kd and ΔL for the five different models. The slope of the quadratic function connecting Kd and ΔL is thus denoted by α_{Kd}^L (Eq. 3).

$$Kd = \alpha_{Kd}^L \cdot \Delta L^2 \qquad (3)$$

For each numerical model with a fixed number of cracks ranging from 4 to 20, five crack disorder realizations are made in the same damaged area of the material, the relationships between the CWI observables and changes of the crack length ΔL are re-established for each group of numerical models in order to calculate the mean value and the standard deviation for the slopes α_θ^L and α_{Kd}^L .

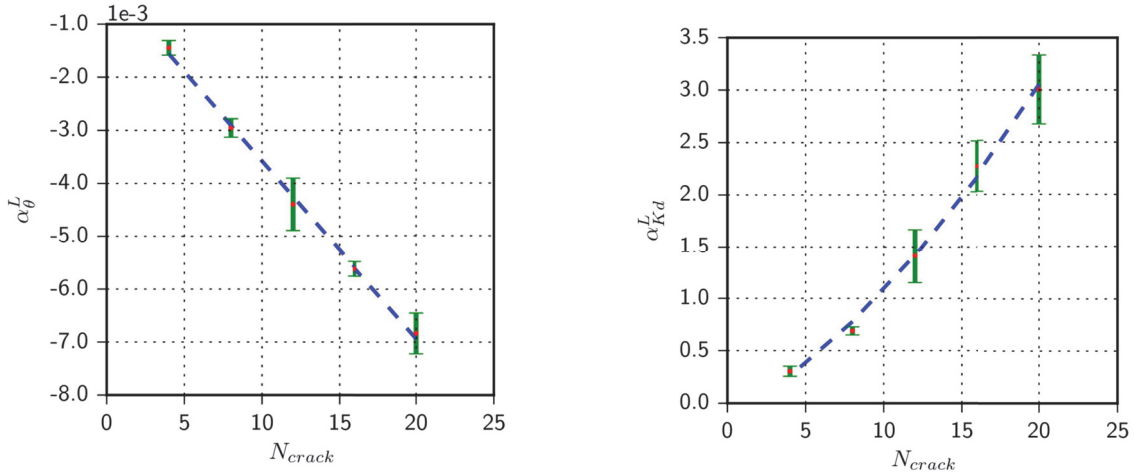

(a) (b)

FIGURE 5. Slopes of CWI observables with the crack length changes in terms of the crack density N_{crack}. Five groups of numerical models are used, each group with a fixed number of random cracks ranging from 4 to 20 in the same damaged area of the material. For each group of models, five realizations of the crack disorder are made in order to get the mean value and the standard deviation of the slope α_θ^L ($\theta \propto L$) and the slope α_{Kd}^L ($Kd \propto L^2$): (a) Slope α_θ^L vs. the crack density N_{crack}; (b) Slope α_{kd}^L vs. N_{crack}.

As shown in Fig. 5 (a), a linear dependence between α_θ^L and the crack density (the number of the cracks) N_{crack} is clearly observed, thus the relative variation of velocity θ can be related to the sum of changes in crack length as follows:

$$\theta = \alpha_{\theta}^{\sum L} \times \left(\sum \Delta L\right) = \alpha_{\theta}^{\sum L} \times \left(\Delta L \times N_{crack}\right) \qquad (4)$$

Similarly, according to Fig. 5 (b), a quadratic function between α_{Kd}^{L} and the crack density N_{crack} can be noted, which gives the following relation between the remnant decorrelation coefficient Kd and the total change in crack length:

$$Kd = \alpha_{Kd}^{\sum L} \times \left(\sum \Delta L\right)^2 = \alpha_{Kd}^{\sum L} \times \left(\Delta L \times N_{crack}\right)^2 \qquad (5)$$

In addition, in Fig. 5 (b), the standard deviation for the values of α_{Kd}^{L} is increasingly important as a function of the crack density. For each realization of crack disorder, the slope α_{Kd}^{L} gives slightly different values, the uncertainty factor between each test is relatively small because the coda waves are multi-diffusing waves, so that a homogeneous wave field after a certain propagation time is obtained. This uncertainty factor arises from the accumulation of changes in the wave trajectories after each interaction with the random cracks: with more cracks in the numerical model, the variations become more important. The standard deviation of α_{Kd}^{L} for the five models of same group is therefore greater for a higher crack density.

CONCLUSIONS

By using the two-dimensional spectral element method (SEM 2D), numerical models with random cracks of random orientations are developed in this paper. Parametric studies are carried out to study the NCWI method, the sensitivity of the CWI observables (the relative variation of velocity θ and the remnant decorrelation coefficient Kd) is studied as a function of different damaged states of materials, which are simulated by slight changes in the length of all cracks in the material. In addition, the sensitivity to crack density (N_{crack}) is studied. The results show that the CWI observables θ and Kd are directly related to the sum of the crack length changes ($\sum_N \Delta L$) in the damaged material and a linear relationship is obtained between θ and $\sum_N \Delta L$, and a quadratic function is observed between Kd and $\sum_N \Delta L$. The reported results constitute another step towards quantification of the damaged materials with more realistic and understandable numerical models. For further steps, the modeling of material damage will be updated to include changes in the intrinsic properties of the material, such as to take into account the nonlinear softening effect, and also the changes in the cracks added to the numerical models Besides, corresponding experiments will be carried out to validate the numerical tests.

ACKNOWLEDGMENTS

This research has been financially supported by the RFI LMAc (Recherche Formation Innovation Le Mans Acoustique) Projet, which in turn is funded by the Région Pays-de-la-Loire (France).

REFERENCES

1. G. Chen, D. Pageot, J.-B. Legland, O. Abraham, M. Chekroun and V. Tournat, "Numerical modeling of ultrasonic coda wave interferometry in a multiple scattering medium with a localized nonlinear defect", *Wave Motion*, vol. 72, pp. 228-243, 2017.
2. Y. Zhang, V. Tournat, O. Abraham, A. Le Duff , B. Lascoup, O. Durand, "Nonlinear mixing of ultrasonic coda waves with lower frequency-swept pump waves for a global detection of defects in multiple scattering media", *J. Appl. Phys.*, vol. 113, pp. 064905, 2013.

3. R. A. Guyer, P. A. Johnson, “Nonlinear mesoscopic elasticity: Evidence for a new class of materials”, *Phys. Today*, vol. 52, pp. 30-36, 1999.
4. J. A. TenCate, “Slow dynamics of earth materials: An example overview”, *Pure Appl. Geophys.*, vol. 168, pp. 2211-2219, 2011.
5. P. Blanloeuil, A. Meziane, A. N. Norris, C. Bacon, “Analytical extension of finite element solution for computing the nonlinear far field of ultrasonic waves scattered by a closed crack”, *Wave Motion*, vol. 66, pp. 132-146, 2016.
6. D. Donskoy, A. Sutin, A. Ekimov, “Nonlinear acoustic interaction on contact interfaces and its use for nondestructive testing”, *NDT & E Int.*, vol. 34, pp. 231-238, 2001.
7. J. -Y. Kim, L. J. Jacobs, J. Qu, J. W. Littles, “Experimental characterization of fatigue damage in a nickel-base super-alloy using nonlinear ultrasonic waves”, J. Acoust. Soc. Am., vol. 120, pp. 1266-1273, 2006.
8. K. Van Den Abeele, P. A. Johnson, A. Sutin, “Nonlinear elastic wave spectroscopy (NEWS) techniques to discern material damage, part I: Nonlinear wave modulation spectroscopy (NWMS)”, *Res. Nondestr. Eval.*, vol. 12, pp. 17-30, 2000.
9. P. A. Johnson, A. Sutin, “Slow dynamics and anomalous nonlinear fast dynamics in diverse solids”, *J. Acoust. Soc. Am.* , vol. 117, pp. 124, 2005.
10. B. Hilloulin, Y. Zhang, O. Abraham, A. Loukili, F. Grondin, O. Durand, V. Tournat, “Small crack detection in cementitious materials using nonlinear coda wave modulation”, *NDT & E Int.*, vol. 68, pp. 98-104, 2014.
11. G. Renaud, J. Rivière, S. Haupert, P. Laugier, “Anisotropy of dynamic acoustoelasticity in limestone, influence of conditioning, and comparison with nonlinear resonance spectroscopy”, J. Acoust. Soc. Am., vol. 133, pp. 3706-3718, 2013.
12. J. N. Eiras, Q. A. Vu, M. Lott, J. Paya, V. Garnier, C. Payan, “Dynamic acoustoelastic test using continuous probe wave and transient vibration to investigate material nonlinearity”, *Ultrasonics*, vol. 69, pp. 29-37, 2016.
13. G. Poupinet, W. Ellsworth, J. Frechet, “Monitoring velocity variations in the crust using earthquake doublets : an application to the calaveras fault, california”, *J. Geophys. Res.*, vol. 89, pp. 5719–5731, 1984.
14. R. Snieder, A Grêt, H. Douma, J. Scales, “Coda wave interferometry for estimating nonlinear behavior in seismic velocity”, *Science*, vol. 295, pp. 2253-2255, 2002.
15. Y. Zhang, O. Abraham, F. Grondin, A. Loukili, V. Tournat, A. L. Duff, B. Lascoup, O. Durand, “Study of stress-induced velocity variation in concrete under direct tensile force and monitoring of the damage level by using thermally-compensated coda wave interferometry”, *Ultrasonics*, vol. 52, pp. 1038-1045, 2012.
16. E. Larose, S. Hall, “Monitoring stress related velocity variation in concrete with a $2*10^{-5}$ relative resolution using diffuse ultrasound”, *J. Acoust. Soc. Am.*, vol. 125, pp. 1853-1856, 2009.
17. Y. Zhang, T. Planès, E. Larose, A. Obermann, C. Rospars, G. Moreau, “Diffuse ultrasound monitoring of stress and damage development on a 15-ton concrete beam”, *J. Acoust. Soc. Am.*, vol. 139, pp. 1691-1701, 2016.
18. D. Komatitsch, J. P. Vilotte, “The spectral element method: an effective tool to simulate the seismic response of 2D and 3D geological structures”, *B. Seismol. Soc. Am.*, vol. 88, pp. 5961-5972, 1998.
19. G. M. Mavko, A. Nur, “Effect of non-elliptical cracks on compressibility of rocks”, *J. Geophys. Res.*, vol. 83, pp. 4459-4468, 1978.